

Atmospheric Processing of Loess Particles in a Polluted Urban Area of Northwestern China

Yang Chen^{1,2} , Huanwu Liu³ , Ru-Jin Huang¹, Fumo Yang⁴, Mi Tian², Xiaojiang Yao², Zhenxing Shen⁵, Lulu Yan⁶, and Junji Cao¹ 

¹State Key Laboratory of Loess and Quaternary Geology (SKLLQG), and Key Laboratory of Aerosol Chemistry and Physics (KLACP), Institute of Earth Environment, Chinese Academy of Sciences, Xi'an, China, ²Chongqing Institute of Green and Intelligent Technology, Chinese Academy of Sciences, Chongqing, China, ³Xi'an Environmental Monitor Station, Xi'an, China, ⁴National Engineering Research Center for Flue Gas Desulfurization, School of Architecture and Environment, Sichuan University, Chengdu, China, ⁵Department of Environmental Sciences and Engineering, Xi'an Jiaotong University, Xi'an, China, ⁶Department of Environmental and Municipal Engineering, Xi'an University of Architecture and Technology, Xi'an, China

Key Points:

- Road and soil dust were major sources of ambient loess particles in Xi'an
- Airborne loess particles were significantly processed in the urban plume
- Nighttime chemistry was important for the uptake of nitrate and chloride to loess particles

Supporting Information:

- Supporting Information S1

Correspondence to:

J. Cao and F. Yang,
cao@loess.llqg.ac.cn;
fumoyang@scu.edu.cn

Citation:

Chen, Y., Liu, H., Huang, R.-J., Yang, F., Tian, M., Yao, X., et al. (2019). Atmospheric processing of loess particles in a polluted urban area of Northwestern China. *Journal of Geophysical Research: Atmospheres*, 124, 7919–7929. <https://doi.org/10.1029/2018JD029956>

Received 9 APR 2018

Accepted 21 MAY 2019

Accepted article online 9 JUL 2019

Published online 22 JUL 2019

Author Contributions:

Formal analysis: Huanwu Liu

Methodology: Xiaojiang Yao

Validation: Xiaojiang Yao

Writing - original draft: Yang Chen

Writing - review & editing: Yang Chen

Abstract Loess is an important dust component of airborne particles in Northwestern China. Knowledge of the chemical composition, mixing state, and processing of loess particles in urban plumes is still limited. Urban loess particles were characterized using a single-particle aerosol mass spectrometer. To understand sources and processing of loess particles, source samples from the road, urban background, soil, construction, and biomass burning ash were collected in the urban areas and characterized. Loess particles were determined as a kind of calcium-silicate-rich ones, which were internally mixed with calcium, silicates, potassium, elemental carbon, organics, ammonium, sulfate, and nitrate. Road and soil were major sources of loess particles. Among the aged loess particles, the average peak areas of taken-up nitrate and sulfate were comparable to that of (Fe+Ca+Al). Diurnal uptake profiles of chloride, sulfate, oxalate, and nitrate on loess particles were analyzed. The nocturnal elevation of chloride occurred significantly due to the uptake of HCl (g). Nighttime nitrate formation occurred prevalently under high relative humidity conditions via the heterogeneous hydrolysis of N₂O₅. The nighttime enrichment of oxalate, which is a marker for aqueous-formatted secondary organic aerosol, was also found. Besides the nighttime chemistry, the daytime photochemical activities were also a drive for the elevations of sulfate, nitrate, and ammonium. Conclusively, the processing of loess particles in polluted urban plumes significantly altered their chemical composition and mixing state.

1. Introduction

Mineral dust particles are lofted from deserts or semiarid areas into the atmosphere with an annual flux of ~2,000 Tg globally (Huneeus et al., 2011; Usher et al., 2003). Dust particles scatter and absorb solar radiation, affecting the radiation budget of the Earth. Light-extinction efficiency of dust particles strongly depends on their physicochemical properties such as morphology, mineralogy, and mixing state, which vary among regions and sources (Ginoux, 2017).

Dust particle could act as media for the atmospheric photochemical activities. Dust surface participates in heterogeneous reactions, including ozone decomposition, nitrogen-dioxide formation, and photolysis (Cwiertny et al., 2008; Krueger et al., 2004). Dust particles could assist NO₂ in oxidizing SO₂ to sulfate during the Chinese air pollution events (Cheng et al., 2016; He et al., 2014). Hygroscopic species could change processed dust particles into droplets where Fenton reaction produces OH radical participating in heterogeneous oxidation (Deguillaume et al., 2005; Gaston et al., 2017; Tobo et al., 2010). Therefore, atmospheric processing of dust particles could shift the tropospheric oxidation capacity, enhance secondary aerosol formation, and affect climate (Tang et al., 2017). Investigating dust processing in polluted urban areas is essential to evaluating the impacts of aged dust particles on visibility, climate, and human health.

Loess is a type of aeolian dust from the Loess Plateau in Northwestern China (Wu et al., 2011). In urban areas of Xi'an (Shaanxi Province, China), the concentration of fugitive loess was up to 66 μg/m³ (Cao et al., 2008; Li et al., 2016; Zhang et al., 2010). When massive haze events occurred during January 2013, loess was up to 46.3% of the total PM_{2.5} (Huang et al., 2014). Studies have focused on the chemical composition and

©2019. The Authors.

This is an open access article under the terms of the Creative Commons Attribution-NonCommercial-NoDerivs License, which permits use and distribution in any medium, provided the original work is properly cited, the use is non-commercial and no modifications or adaptations are made.

mineralogy of loess, but its processing in urban plumes is inadequately understood (Liu et al., 2004; Wang et al., 2006; Wu et al., 2011).

Single-particle mass spectrometers have been widely used for characterizing size-resolved chemical composition and mixing state of ambient particles (Gard et al., 1997; Li et al., 2011; Zelenyuk et al., 2015). Dust particles from southern California (Silva et al., 2000), Saharan (Dall'Osto et al., 2010), and Asian outflow (Sullivan, Guazzotti, Sodeman, & Prather, 2007) have been examined. In polluted urban areas, dust particles in Mexico City (Moffet et al., 2008), Athens (Dall'osto & Harrison, 2006), and Beijing, Chongqing, and Guangzhou in China (Chen et al., 2017; Li et al., 2014; Tao et al., 2011; Zhang et al., 2014) have been reported. However, few of these online measurements converged on the atmospheric processing of loess particles.

This study aims to characterize the processed, urban loess particles in Northwestern China. The ambient loess particles were compared to the source samples (e.g., road, soil, loess, and construction dust) for studies of origins and processing. Results from this study would improve our understanding of the evolution of loess particles and our capability in assessing the impact on air quality, climate, and human health.

2. Materials and Methods

2.1. Field Measurement and Instrumentation

A single-particle aerosol mass spectrometer (SPAMS) was deployed in an urban area of Xi'an from 26 September 2013 to 13 October 2013. The field observation site is located 10 m above the ground on the rooftop of a building (108.89°E, 34.23°N; Chen et al., 2016). The technical description of SPAMS is available elsewhere (Li et al., 2011). Briefly, SPAMS measures single-particle chemical composition in a size range of 0.2–2.0 μm . The sampled particles pass through an aerodynamic lens and form a narrow beam for sizing. The time of flight of particles crossing two prepositioned 532-nm lasers is used to calculate the vacuum aerodynamic diameter (D_{va}). Sized particles are then decomposed and ionized by a 266-nm laser (2 mJ per shot) and formed both positive and negative ions, which are then analyzed by a dual polarity time-of-flight mass spectrometer. Particulate size distribution is calibrated using the standard National Institute of Standards and Technology (NIST)-traceable polystyrene latex standard (Duke Scientific Inc., USA) before and after the observation. In addition, trace gases (NO_x , ozone, CO, and SO_2) and meteorological parameters are also recorded using instrumentation from Thermo Inc. and Vaisala (MAWS20), respectively. All the data were collected and stored in local time (Beijing time, UTC+8).

2.2. Collection and Analysis of Source Dust Samples

The Xi'an city is located in a semiarid area where the dust could be lofted from the naked surfaces like roads, farms, and naked surfaces in the city. As a rapid-developing city, Xi'an had at least 3,000 work-in building yards in the urban area (Long et al., 2016). Therefore, a series of source samples, including soil, road, construction, urban background, biomass burning (BB) ash, and authentic loess samples, were collected and analyzed for source identification and comparison. Sixteen soil samples were collected from 16 farmland locations near the city (see Table S1 in the supporting information for details). One soil sample was collected at each site unless otherwise mentioned. Soil from the surface to a depth of 10 cm was collected, and the samples were settled into a zip bag for cryostorage. Twenty-five samples were collected on many urban roads, including primary, secondary, and branch roads (Table S2). The samples of city background and construction dust were acquired from the Drum Tower (a historical landscape, 108.95°E, 34.27°N) and a constructing yard (109.09°E, 34.19°N), respectively. The road, city background dust, and construction samples were collected from the surface dirt. BB ash samples were acquired from the chimney of a BB boiler located in the Chengtai Paper Industry (120.53°E, 31.24°N). The authentic standard loess (Product ID GBW07454 GSS-25) was purchased from the Chinese Standard Material Center.

All samples were dried at room temperature before resuspension for resampling and laboratory analyses. All soil samples were mixed with a blender, and the mixture was sieved through Tyler 30, 50, 100, 200, and 400 mesh sieves. Five grams of the sieved mixture was placed in a 1-L extraction bottle. Zero air was pumped in the bottle at a flow rate of 5 L/min; then the soil powder was blown to a 500-L chamber for mixing. The resuspended particles were then analyzed using a SPAMS. The resuspension system was cleaned after use to avoid contamination.

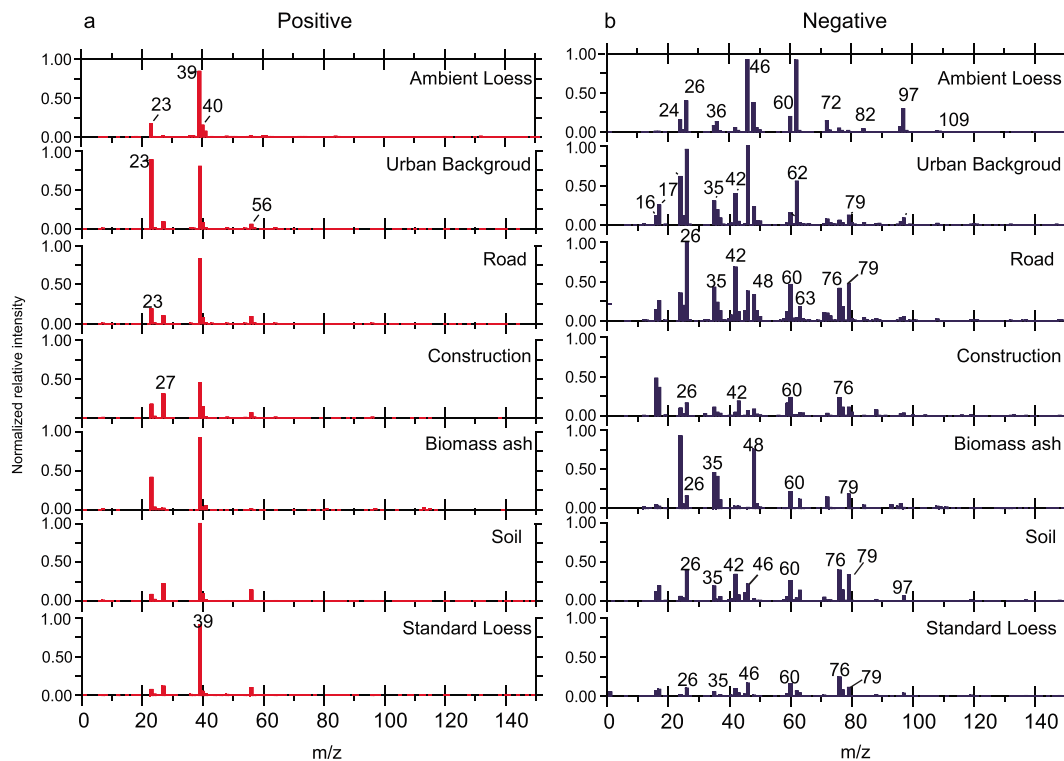


Figure 1. Average positive (a) and negative (b) mass spectra for ambient loess, urban background dust (20,367 particles), road dust (15,673 particles), construction (5,076 particles), biomass burning ash (7,832 particles), local soil (10,672 particles), and authentic loess (3,547 particles).

2.3. Data Analysis

During the field observation, 137,748 particles with validated mass spectra were collected. A query combination of Ca^+ (m/z 40), $[\text{SiO}_2]^-$ (m/z -60), and $[\text{SiO}_3]^-$ (m/z -76) was used to search the SPAMS data set for the dust particles. The query resulted in 46,834 particles (34.0% in number). Since a proportion of particles could not be assigned to dust (e.g., BB particles), thus a clustering algorithm (Adaptive Resonance Theory Neural network, ART-2a) was applied to resolve particle types from the query (Song et al., 1999). A learning rate of 0.05, a vigilance factor of 0.70, and 20 iterations were used. Four unique particle clusters, namely, an aged BB (34%), a Ca-ECOC type (4%), a Ca-EC type (4%), and a major Ca-Si type (58%; Figure S2), were resolved. The major Ca-Si particles, which were mainly composed of Ca^+ , SiO_2^- , SiO_3^- , and PO_3^- , were assigned to dust.

3. Results and Discussion

3.1. Characterization of Ambient and Source Dust Particles

Figure 1 shows the average mass spectra of ambient dust, urban background, soil, construction, road, BB ash, and the authentic loess. The assignment of ions in each mass spectrum is shown in Table S3. Coefficient of determination (R^2) was calculated using the relative ion peak areas among different mass spectra. Relative peak areas of sulfate (m/z -80 and -97) and nitrate (m/z -46 and -62) were excluded because their strong ion intensity could cause significant bias on the R^2 calculation. As shown in Table 1, the mass spectra of ambient dust particles had high R^2 values (0.92, 0.89, and 0.88) with those of road dust, soil, and standard loess, respectively. Ambient dust was also similar to urban background dust ($R^2 = 0.57$) and construction dust ($R^2 = 0.63$). The source samples had good correlations with each other. For example, authentic loess was identical to soil ($R^2 = 0.99$) and road dust ($R^2 = 0.94$). These results suggest that road and soil dust were the principal sources of ambient dust particles. As a result of this, we used the term “ambient loess” to describe the ambient dust particles in Xi’an.

Among multiple mass spectra, the relative intensity of the major ions varied, as shown in Figure 1a. The ambient loess had a K^+/Ca^+ ratio of 10, which was consistent with a previous study in Xi’an (Chen et al.,

Table 1
Coefficients of Determination (R^2) Between Mass Spectra of Ambient Loess Particles and Source Samples

	Ambient	Urban Bkd	Soil	BB ash	Construction	Loess	Road
Ambient	1.00						
Urban Bkd	0.57	1.00					
Soil	0.89	0.50	1.00				
BB ash	0.80	0.76	0.72	1.00			
Construction	0.63	0.55	0.71	0.57	1.00		
Loess	0.88	0.50	0.99	0.72	0.71	1.00	
Road	0.92	0.67	0.96	0.83	0.72	0.94	1.00

Note. BB biomass burning; Bkd = background dust.

2016). The K^+/Ca^+ values of urban background dust, soil, construction, loess, and road particles were 12, 15, 35, 10, and 11, respectively. The result is different from previous single-particle studies. For example, K^+/Ca^+ values of dust were 1.0 in Beijing (Li et al., 2014), 0.75 in Shanghai (Yang et al., 2009), ~2 for Asian dust (Furutani et al., 2011), and ~1.3 for Sahara dust (Dall'Osto et al., 2010). There are several possible reasons. First, the ion peak areas could be affected by chemical species in the particle matrix. Second, variations of laser energy might vary ion peak areas. Third, dust mineralogy also influenced laser desorption/ionization efficiency (Allen et al., 2000; Bhawe et al., 2002; Gross et al., 2000). Hereby, we recommend a K^+/Ca^+ of 10 for loess particles in SPMS studies.

Elemental Carbon (EC) components ($C_2^- - C_6^-$) were also abundant in ambient loess, urban background, biomass ash, and authentic loess. EC was ordinarily from combustion including diesel, gasoline, and biomass (Ault et al., 2010; Gaston et al., 2013; Spencer & Prather, 2006; Toner et al., 2008). Loess particles could coagulate with combustion species (more discussion in section 3.2 below), as has been reported in Shanghai (Yang et al., 2009) and on Sahara dust particles (Dall'Osto et al., 2010). Soil samples were rich in EC because straw burning has been prevalent in the Guanzhong Basin for thousands of years, and burning residues were well mixed with soil. Additionally, in the construction dust, high signal of O^- ($m/z -16$), OH^- ($m/z -17$), $[SiO_2]^-$ ($m/z -60$), $[SiO_3]^-$ ($m/z -76$), $[CN]^-$, and $[CNO]^-$ were found because concrete powder contains metal oxides such as CaO, Fe_xO_y , Al_2O_3 , and MgO (Goodman et al., 2001). When broken up under laser, these metal oxides could cause high signals of $[O]^-$ and $[OH]^-$.

A ternary plot was composed to evaluate the secondary uptake on loess particles by comparing with source samples (Sullivan, Guazzotti, Sodeman, & Prather, 2007). In the ternary plot, the sum-up average peak areas of (Fe+Ca+Al) was used to represent the intensity of the mineral species, sulfate, and nitrate to indicate that of secondary species. If a kind of dust particles had insignificant secondary uptake, they should be close to the (Fe+Ca+Al) vertex; otherwise, the positions of the particle type should be close to the vertexes of sulfate and nitrate. As shown in Figure 2, construction, authentic loess, BB ash, and soil samples had minimum uptake of sulfate and nitrate, while road and urban background samples had large amounts of sulfate and nitrate. For ambient loess particles, dramatic uptake of sulfate and nitrate was observed with the mass ratios of nitrate:sulfate:(Fe+Ca+Al) being 53%:18%:29%, while the ratios in authentic loess were 2%:2%:96%. These results suggest that nitrate and sulfate uptake significantly altered the chemical composition of airborne loess particles.

Figure S3 shows the unscaled size distribution of ambient particles and source samples. Note that all the source dust samples were resuspended. Thus, their size distribution could be different from the real distributions (Allen et al., 2000; Qin et al., 2006). The ambient loess particles had a wide distribution and peaked around 0.64–0.72 μm while the source profiles

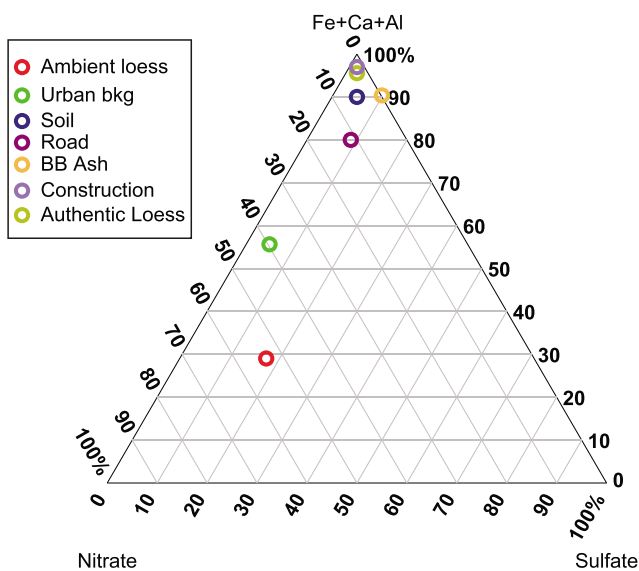


Figure 2. Ternary plot of the average peak area of sulfate, nitrate, and (Fe+Ca+Al) of ambient loess, city background dust, soil, road dust, and biomass burning (BB) ash. The vertex of Fe+Ca+Al suggests that nitrate is 100% in this position.

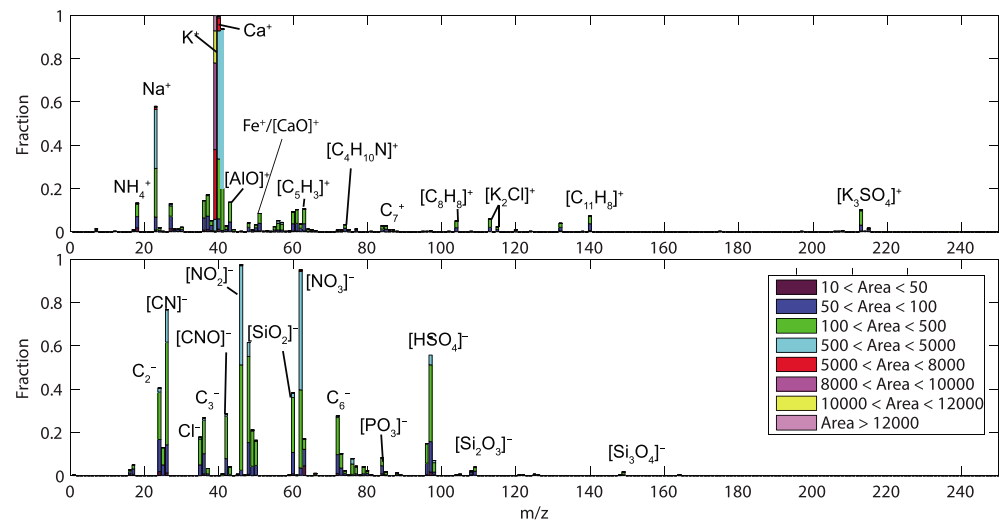


Figure 3. Average digital mass spectra of ambient loess particles in Xi'an.

had sharp size distributions when D_{va} was larger than $0.50 \mu\text{m}$. Soil dust peaked at $0.72 \mu\text{m}$, and standard loess, road, and BB ash peaked at $0.74 \mu\text{m}$. These results suggest that the atmospheric processing majorly changed the size distribution of loess particles with $D_{va} < 0.7 \mu\text{m}$.

3.2. Mixing State Analysis

Mixing state of ambient loess particles is shown in a digital average mass spectrum (Figure 3). Each ion peak represents its fraction in the particle matrix, and the color maps indicate the corresponding ion peak area ranges (Sullivan, Guazzotti, Sodeman, & Prather, 2007). Among all the species, K^+ was the most abundant with a ratio of 1.00, followed by Ca^+ (0.97) and Na^+ (0.62). Aluminum ions such as Al^+ (m/z 27) and $[\text{AlO}]^+$ were detected with ratios of 0.13 and 0.14, respectively. $[\text{CaO}]^+ / [\text{Fe}]^+$ ion has a fraction of 0.05. NH_4^+ (m/z 18) and $[\text{K}_2\text{Cl}]^+$ (m/z 113 and 115) were observed. Low fractions of organic ion markers, such as $[\text{C}_4\text{H}_3]^+$ (m/z 51), $[\text{C}_5\text{H}_3]^+$ (m/z 63), and $[\text{C}_{11}\text{H}_8]^+$ (m/z 140), were also detected. In the negative mass spectra, nitrate was predominant, along with $[\text{PO}_3]^-$, $[\text{CN}]^-$, and $[\text{CNO}]^-$. Mineral components, such as $[\text{SiO}_2]^-$, $[\text{SiO}_3]^-$, $[\text{Si}_2\text{O}_3]^-$, and $[\text{Si}_3\text{O}_4]^-$, were also present. Overall, the urban loess particles were a mixture of mineral species, organic species, sulfate, chloride, and nitrate. Moreover, the result is consistent with what was previously found (Chen et al., 2016).

The atmospheric aging process could alter mixing state of loess particles. In this section, comparisons between ambient loess particles and source samples were conducted to illustrate the particulate aging degrees. Distributions (mixing ratio and the corresponding ion intensity) of markers, that is, $[\text{HSO}_4]^-$, $[\text{NO}_3]^-$, $[\text{NH}_4]^+$, $[\text{CNO}]^-$, $[\text{Cl}]^-$, $[\text{PO}_3]^-$, and oxalate on both ambient loess particles and source samples, are shown in Figures 4 and 5, respectively. Sulfate, nitrate, and ammonium were abundant in not only ambient loess particles but also the urban background samples. Respectively, 84%, 97%, and 51% of urban background particles contained sulfate, nitrate, and ammonium. As expected, the urban background dirt is a sink of ambient Particulate Matter (PM) due to high mixing ratios of secondary species. As shown in Figure 5, ambient loess particles contained the most vigorous relative ion intensity of $[\text{HSO}_4]^-$, $[\text{NO}_3]^-$, and $[\text{NH}_4]^+$, followed by urban background samples. Additionally, road dust was also both a source and a sink of urban PM, containing strong signals of $[\text{HSO}_4]^-$, $[\text{NO}_3]^-$, and $[\text{NH}_4]^+$. These results also suggest that urban background particles were also a sink for atmospheric ammonia.

$[\text{CNO}]^-$ is commonly used as a marker of organic nitrogen species in single-particle studies (Angelino et al., 2001). In the atmosphere, organic nitrogen species are represented by RNO_2 species when their organic precursor reacted with NO_x (Seinfeld & Pandis, 2016). Organic nitrogen species could also be emitted from BB (Silva et al., 1999) or biological activities (Creamean et al., 2016). The mixing fractions of $[\text{CNO}]^-$ were in the order of road (0.86) > soil (0.84) > loess (0.77) > urban background (0.51) > BB ash (0.41) > construction (0.40). This result indicates that CNO^- was widely distributed in multiple sources. For example, the soil

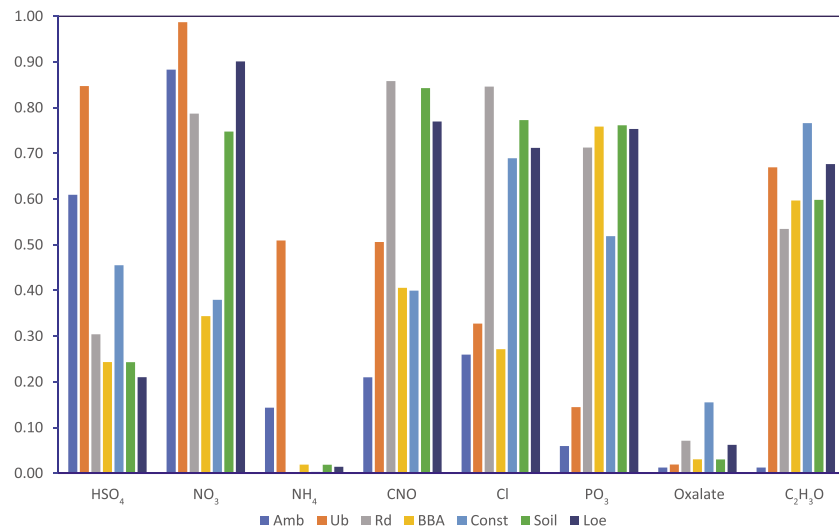


Figure 4. Mixing fraction of major ion species in different types of dust particles.

organic nitrogen could be from microorganisms and humic-like substances, while that in the road and urban background dust could be from combustion or photochemical activities (Dall’Osto et al., 2010). During the atmospheric processing, [CNO]⁻ on ambient loess particles decreased dramatically due to the photochemical removal, that is, photolysis (Healy et al., 2012).

Cl⁻ can be primarily released into the atmosphere via BB, biological activities, and waste incineration (Chen et al., 2016; Zhang et al., 2011). HCl(g) can then be formed when the primary chloride reacted with gaseous acidic species such as H₂SO₄ (g) and HNO₃ (g; Moffet et al., 2008). Uptake of HCl (g) can be a secondary

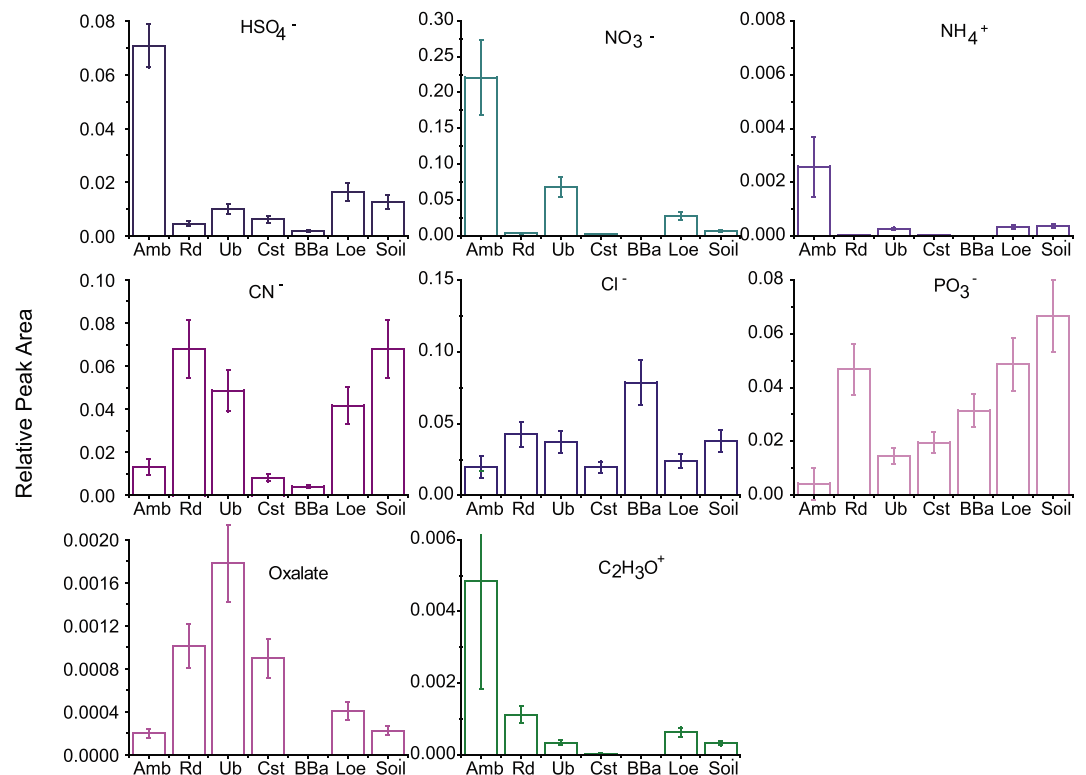


Figure 5. Normalized peak area for ion markers in each source cluster. Amb stands for ambient, Ub for urban background, Rd for road, BBa for biomass burning ash, Const for construction, and Loe for loess.

source of Cl^- on dust particles. The mixing ratio of Cl^- followed the order of road (0.85) > soil (0.84) > loess (0.77) > construction (0.69) > urban background (0.33) > BB ash (0.27) > ambient (0.18). The high mixing ratio of Cl^- in construction particles is probably due to oxides in concrete, such as CaO , Al_2O_3 , and MgO , which strongly absorb HCl (g; Goodman et al., 2001). The low mixing ratio of Cl^- in ambient loess was due to the removal of HCl (g) when Cl^- reacted with H^+ (Seinfeld & Pandis, 2016).

PO_3^- is an important component of soil dust or from the biological residues (Creamean et al., 2013). $[\text{PO}_3]^-$ had similar fractions in the road (0.71), soil (0.76), BB ash (0.76), and the authentic loess (0.75). However, the distribution of PO_3^- in ambient loess was much lower than that of in source samples, which could be caused by the matrix effect in single particle studies (Gross et al., 2000). Oxalate is commonly used as a marker of secondary organic aerosol (SOA) formed in the aqueous phase (Ervens et al., 2011), but it could also be from BB (Falkovich et al., 2005). Oxalate was widely distributed in soil and loess due to fungi activities (Dutton & Evans, 1996). To sum up, uptake of secondary species on loess particles could alter their physicochemical properties significantly when crossing urban plumes. In the next section, the diurnal evolution of loess particles was illustrated.

3.3. Diurnal Profile of Secondary Species on Dust Particles

Uptake of nitrate, sulfate, and chloride on dust particles has been reported in literature (Moffet et al., 2008; Sullivan, Guazzotti, Sodeman, Tang, et al., 2007; Sullivan, Guazzotti, Sodeman, & Prather, 2007; Sullivan & Prather, 2007). In this work, we investigated the diurnal uptake of nitrate, sulfate, ammonium, and chloride on loess particles. Since the arbitrary relative sensitivities factor was unavailable for SPAMS, we used ratios of ion peak area of SO_4^- , NO_3^- , NH_4^+ , and Cl^- in dust particle data set to illustrate the quantities of these species, and the peak area of m/z 40 (Ca^+) was used to normalize the shot-to-shot variations of the laser energy absorbed by each dust particle (Sullivan, Guazzotti, Sodeman, & Prather, 2007). During the observation, wind was mostly from south of the sampling site (Figure S1) with an average speed of 1.5 m/s. Thus, the collected loess particles were mainly locally aged. Therefore, when discussing diurnal profiles of secondary uptake, it is worth to mention the diurnal behavior of relative humidity (RH). As shown in Figure 6a, RH remained at high levels with a median value of ~80% in the nighttime and decreased to 40% in the afternoon (14:00, local time, UTC+8, and hereafter). RH was sufficiently high during the nighttime that could change the hygroscopic species such as $(\text{NH}_4)_2\text{SO}_4$, NH_4NO_3 , and NH_4Cl into droplets, providing media for aqueous reactions on loess particles (Tobo et al., 2010). The temporal trends of $[\text{NO}_3^-]/\text{Ca}^+$, $[\text{HSO}_4^-]/\text{Ca}^+$, Cl^-/Ca^+ , $[\text{NH}_4^+]/\text{Ca}^+$, and Oxalate/ Ca^+ are available in Figure S4. As expected, $[\text{NH}_4^+]/\text{Ca}^+$ had good correlations with $[\text{HSO}_4^-]/\text{Ca}^+$ and $[\text{NO}_3^-]/\text{Ca}^+$ with R values of 0.67 and 0.86 respectively.

As shown in Figure 6, $[\text{NO}_3^-]/\text{Ca}^+$ had an early morning peak around 4:00; this peak possibly occurred via $\text{NO}_3/\text{N}_2\text{O}_5 + \text{H}_2\text{O}$ pathway on dust particles (Wang, Lu, et al., 2017; Zhang et al., 2015). In the daytime, $[\text{NO}_3^-]/\text{Ca}^+$ had a noon peak (12:00) driven by the uptake of HNO_3 (g) produced via gas phase $\text{OH} + \text{NO}_2$ pathway. HNO_3 (g) could convert to $\text{Ca}(\text{NO}_3)_2$ when reacting with CaCO_3 on the loess particles (Sullivan et al., 2005). The absorptive condensation of NH_4NO_3 (g) could also lead to the $[\text{NO}_3^-]/\text{Ca}^+$ nitrate elevation. A diurnal arising of particulate NH_4NO_3 had been observed in a similar season (Wang, Huang, et al., 2017). In a previous study, an elevation of NH_4NO_3 particle was observed at noon in California, USA, where the air stagnation was also common (Qin et al., 2012). Additionally, the diurnal profile of $[\text{NH}_4^+]/\text{Ca}^+$ was consistent with that of $[\text{NO}_3^-]/\text{Ca}^+$ in the daytime, suggesting that the gas/particle partitioning of NH_4NO_3 was the major pathway for uptake of nitrate and ammonium.

Uptake of H_2SO_4 (g) on dust particles has been studied elsewhere (Tang et al., 2016). As shown in Figure 6c, the diurnal profile of $[\text{HSO}_4^-]/\text{Ca}^+$ showed peaks at 5:00 and remained at high levels until 16:00. The 5:00 peak could be produced by the heterogeneous oxidation of S (IV) to S (VI) by H_2O_2 or other hydroperoxide species when relative humidity was high (Tang et al., 2016; Usher et al., 2002). $[\text{HSO}_4^-]/\text{Ca}^+$ remained high after the morning rush hours when the concentration of NO_2 was high. SO_2 and NO_2 can rapidly react with each other on the dust surface to form sulfate (He et al., 2014). In the daytime NH_4SO_4 produced from H_2SO_4 (g) and ammonia could be necessary for the afternoon peak of $[\text{HSO}_4^-]/\text{Ca}^+$.

The urban area of Xi'an is rich in gaseous and particulate chloride emitted from industry, waste incineration, and BB (Chen et al., 2016). The gas phase HCl (g) could be generated from the reaction between chloride and

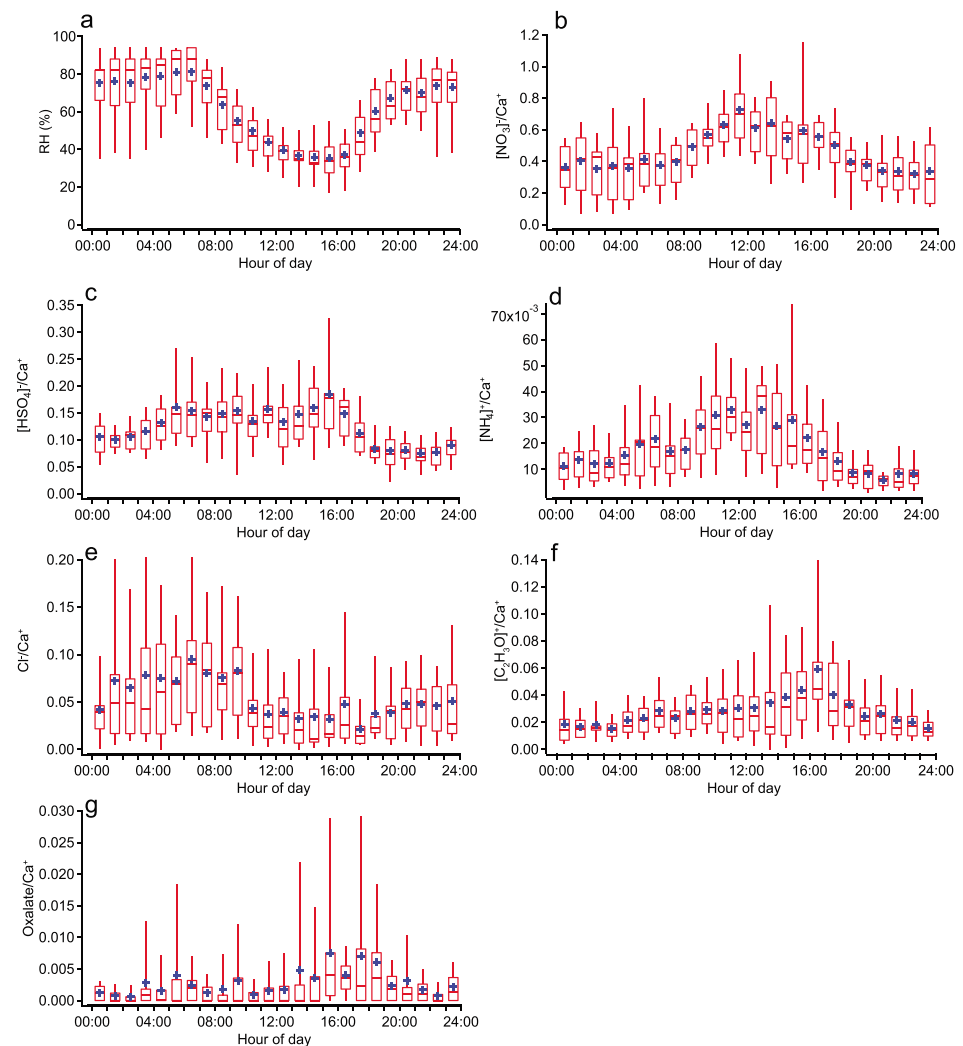


Figure 6. Diurnal profiles of (a) RH, (b) $[\text{NO}_3^-]/\text{Ca}^+$, (c) $[\text{HSO}_4^-]/\text{Ca}^+$, (d) $[\text{NH}_4^+]/\text{Ca}^+$, (e) Cl^-/Ca^+ , (f) $[\text{C}_2\text{H}_3\text{O}]^+/\text{Ca}^+$, and (g) $\text{Oxalate}/\text{Ca}^+$.

strong acids such as H_2SO_4 (g) and HNO_3 (g) on the dust surface. Dust particles acting as a sink of HCl (g) in the marine boundary layer have been reported, but no clear diurnal pattern was acquired due to limitations of ship measurement (Sullivan, Guazzotti, Sodeman, Tang, et al., 2007). Cl^-/Ca^+ remained at high levels in the dark possibly due to the uptake of HCl (g) and its reaction with CaCO_3 as well as other metal oxides (Sullivan, Guazzotti, Sodeman, Tang, et al., 2007). The diurnal Cl^-/Ca^+ decreased dramatically after 8:00 due to the removal of volatile HCl (g) as aforementioned (Faxon & Allen, 2013; Gard et al., 1998). Also, the daytime uptake of HCl (g) could be weak because HCl (g) could be oxidized rapidly in the troposphere (Finlayson-Pitts & Pitts, 2000).

The diurnal condensation of oxalate on dust in the marine environment has been reported by Sullivan and Prather (2007), and they also proposed that the gas-particle phase partitioning of oxalic acid was important. In this study, as shown in Figure 6g, $\text{Oxalate}/\text{Ca}^+$ showed a three-spike diurnal pattern peaking at 3:00, 5:00, and 17:00. The aqueous oxidation of glyoxal by OH , H_2O_2 , and other peroxides could drive the nighttime elevation of oxalate in the dust droplets (Tang et al., 2017). The nighttime peak of oxalate has been observed by Sullivan and Prather (2007), but they proposed that the peak was majorly caused by long-range transport. Moreover, the oxalate formation was controlled by aerosol acidity of dust particles (Ervens et al., 2011). As shown in Figure 6c, oxalate became maximum when HSO_4^-/Ca was the highest ($R = 0.53$; Figure S4). Overall, to our best knowledge, this part is novel for reporting the diurnal uptake of nitrate, sulfate,

semivolatile-SOA, and aqueous SOA on loess, and we reveal that the nighttime chemistry was essential for the nitrate and chloride uptake.

4. Conclusions

The atmospheric processing of loess particles in urban areas of Xi'an was studied by comparing the ambient loess particles to the source samples collected from the urban background, road, soil, construction, BB ash, and authentic loess. Road and soil were apportioned as the major sources of ambient loess particles. Urban airborne loess particles were found to be significantly processed via the uptake of secondary pollutants such as organics, sulfate, nitrate, and ammonium. The diurnal uptake behaviors of chloride, sulfate, and nitrate were investigated. Both daytime and nighttime chemistry played essential roles on the secondary uptake on loess particles. Heterogeneous hydrolysis of N_2O_5 was the major pathway for the elevation of nitrate in the nighttime. Results from this study could be utilized in model studies to evaluate the impact of aged dust particles on human health, visibility, and air quality.

Acknowledgments

Financial support from the National Natural Science Foundation of China (Grant 41703136) and the National Key Research and Development Program of China (2016YFC0200405) are acknowledged. Data supporting this paper can be found at <http://doi.org/10.5281/zenodo.3237973> and is also indexed at OpenAIRE (<https://explore.openaire.eu/search/dataset?datasetId=r37b0ad08687:9e7-ca1d421b3c86b0fb9859dae51ebaf>). The authors declare no competing financial interests.

References

- Allen, J. O., Fergenson, D. P., Gard, E. E., Hughes, L. S., Morrical, B. D., Kleeman, M. J., et al. (2000). Particle detection efficiencies of aerosol time of flight mass spectrometers under ambient sampling conditions. *Environmental Science & Technology*, *34*(1), 211–217. <https://doi.org/10.1021/es9904179>
- Angelino, S., Suess, D. T., & Prather, K. A. (2001). Formation of aerosol particles from reactions of secondary and tertiary alkylamines: characterization by aerosol time-of-flight mass spectrometry. *Environmental Science and Technology*, *35*(15), 3130–3138. <https://doi.org/10.1021/es0015444>
- Ault, A. P., Gaston, C. I., Wang, Y., Dominguez, G., Thiemens, M. H., & Prather, K. a. (2010). Characterization of the single particle mixing state of individual ship plume events measured at the Port of Los Angeles. *Environmental Science & Technology*, *44*(6), 1954–1961. <https://doi.org/10.1021/es902985h>
- Bhave, P. V., Kleeman, M. J., Allen, J. O., & Hughes, L. S. (2002). Evaluation of an air quality model for the size and composition of source-oriented particle classes. *Environmental Science & Technology*, *36*(10), 2154–2163. <https://doi.org/10.1021/es0112700>
- Cao, J. J., Chow, J. C., Watson, J. G., Wu, F., Han, Y. M., Jin, Z., et al. (2008). Size-differentiated source profiles for fugitive dust in the Chinese Loess Plateau. *Atmospheric Environment*, *42*(10), 2261–2275. <https://doi.org/10.1016/j.atmosenv.2007.12.041>
- Chen, Y., Cao, J., Huang, R., Yang, F., Wang, Q., & Wang, Y. (2016). Characterization, mixing state, and evolution of urban single particles in Xi'an (China) during wintertime haze days. *Science of the Total Environment*, *573*, 937–945. <https://doi.org/10.1016/j.scitotenv.2016.08.151>
- Chen, Y., Yang, F., Mi, T., Cao, J., Shi, G., Huang, R., et al. (2017). Characterizing the composition and evolution of and urban particles in Chongqing (China) during summertime. *Atmospheric Research*, *187*, 84–94. <https://doi.org/10.1016/j.atmosres.2016.12.005>
- Cheng, Y., Zheng, G., Wei, C., Mu, Q., Zheng, B., Wang, Z., et al. (2016). Reactive nitrogen chemistry in aerosol water as a source of sulfate during haze events in China. *Science Advances*, *2*(12), e1601530. <https://doi.org/10.1126/sciadv.1601530>
- Creamean, J. M., Suski, K. J., Rosenfeld, D., Cazorla, A., DeMott, P. J., Sullivan, R. C., et al. (2013). Dust and biological aerosols from the Sahara and Asia influence precipitation in the western U. S. *Science*, *339*(6127), 1572–1578. <https://doi.org/10.1126/science.1227279>
- Creamean, J. M., White, A. B., Minnis, P., Palikonda, R., Spangenberg, D. A., & Prather, K. A. (2016). The relationships between insoluble precipitation residues, clouds, and precipitation over California's southern Sierra Nevada during winter storms. *Atmospheric Environment*, *140*, 298–310. <https://doi.org/10.1016/j.atmosenv.2016.06.016>
- Cwiertny, D. M., Young, M. A., & Grassian, V. H. (2008). Chemistry and photochemistry of mineral dust aerosol. *Annual Review Of Physical Chemistry*, *59*(1), 27–51. <https://doi.org/10.1146/annurev.physchem.59.032607.093630>
- Dall'osto, M., & Harrison, R. (2006). Chemical characterisation of single airborne particles in Athens (Greece) by ATOFMS. *Atmospheric Environment*, *40*(39), 7614–7631. <https://doi.org/10.1016/j.atmosenv.2006.06.053>
- Dall'Osto, M., Harrison, R. M., Highwood, E. J., O'Dowd, C., Ceburnis, D., Querol, X., & Achterberg, E. P. (2010). Variation of the mixing state of Saharan dust particles with atmospheric transport. *Atmospheric Environment*, *44*(26), 3135–3146. <https://doi.org/10.1016/j.atmosenv.2010.05.030>
- Deguillaume, L., Leriche, M., Desboeufs, K., Mailhot, G., George, C., & Chaumerliac, N. (2005). Transition metals in atmospheric liquid phases: Sources, reactivity, and sensitive parameters. *Chemical Reviews*, *105*(9), 3388–3431. <https://doi.org/10.1021/cr040649c>
- Dutton, M. V., & Evans, C. S. (1996). Oxalate production by fungi: Its role in pathogenicity and ecology in the soil environment. *Canadian Journal of Microbiology*, *42*(9), 881–895. <https://doi.org/10.1139/m96-114>
- Ervens, B., Turpin, B. J., & Weber, R. J. (2011). Secondary organic aerosol formation in cloud droplets and aqueous particles (aqSOA): a review of laboratory, field and model studies. *Atmospheric Chemistry and Physics*, *11*(21), 11,069–11,102. <https://doi.org/10.5194/acp-11-11069-2011>
- Falkovich, A. H., Graber, E. R., Schkolnik, G., Rudich, Y., Maenhaut, W., & Artaxo, P. (2005). Low molecular weight organic acids in aerosol particles from Rondônia, Brazil, during the biomass-burning, transition and wet periods. *Atmospheric Chemistry and Physics*, *5*(3), 781–797. <https://doi.org/10.5194/acp-5-781-2005>
- Faxon, C. B., & Allen, D. T. (2013). Chlorine chemistry in urban atmospheres: A review. *Environmental Chemistry*, *10*(3), 221–233. <https://doi.org/10.1071/en13026>
- Finlayson-Pitts, B. J., & Pitts, J. N. (2000). *Chemistry of the upper and lower atmosphere: Theory, experiments, and applications*. London: Academic Press.
- Furutani, H., Jung, J., Miura, K., Takami, A., Kato, S., Kajii, Y., & Uematsu, M. (2011). Single-particle chemical characterization and source apportionment of iron-containing atmospheric aerosols in Asian outflow. *Journal of Geophysical Research*, *116*, D18204. <https://doi.org/10.1029/2011JD015867>

- Gard, E., Mayer, J. E., Morrical, B. D., Dienes, T., Fergenson, D. P., & Prather, K. A. (1997). Real-time analysis of individual atmospheric aerosol particles: Design and performance of a portable ATOFMS. *Analytical Chemistry*, *69*(20), 4083–4091. <https://doi.org/10.1021/ac970540n>
- Gard, E. E., Kleeman, M. J., Gross, D. S., Hughes, L. S., Allen, J. O., Morrical, B. D., et al. (1998). Direct observation of heterogeneous chemistry in the atmosphere. *Science*, *279*(5354), 1184–1187. <https://doi.org/10.1126/science.279.5354.1184>
- Gaston, C. J., Pratt, K. A., Suski, K. J., May, N. W., Gill, T. E., & Prather, K. A. (2017). Laboratory studies of the cloud droplet activation properties and corresponding chemistry of saline playa dust. *Environmental Science and Technology*, *51*(3), 1348–1356. <https://doi.org/10.1021/acs.est.6b04487>
- Gaston, C. J., Quinn, P. K., Bates, T. S., Gilman, J. B., Bon, D. M., Kuster, W. C., & Prather, K. A. (2013). The impact of shipping, agricultural, and urban emissions on single particle chemistry observed aboard the R/VAtlantis during CalNex. *Journal of Geophysical Research: Atmospheres*, *118*, 5003–5017. <https://doi.org/10.1002/jgrd.50427>
- Ginoux, P. (2017). Warming or cooling dust? *Nature Geoscience*, *10*(4), 246–248. <https://doi.org/10.1038/ngeo2923>
- Goodman, A. L., Bernard, E. T., & Grassian, V. H. (2001). Spectroscopic study of nitric acid and water adsorption on oxide particles: Enhanced nitric acid uptake kinetics in the presence of adsorbed water. *The Journal of Physical Chemistry A*, *105*(26), 6443–6457. <https://doi.org/10.1021/jp003722l>
- Gross, D. S., Galli, M. E., Silva, P. J., & Prather, K. A. (2000). Relative sensitivity factors for alkali metal and ammonium cations in single-particle aerosol time-of-flight mass spectra. *Analytical Chemistry*, *72*(2), 416–422. <https://doi.org/10.1021/ac990434g>
- He, H., Wang, Y., Ma, Q., Ma, J., Chu, B., Ji, D., et al. (2014). Mineral dust and NOx promote the conversion of SO2 to sulfate in heavy pollution days. *Scientific Reports*, *4*(1), 4172. <https://doi.org/10.1038/srep04172>
- Healy, R. M., Chen, Y., Kourtchev, I., Kalberer, M., O'Shea, D., Wenger, J. C., & O'Shea, D. (2012). Rapid formation of secondary organic aerosol from the photolysis of 1-nitronaphthalene: Role of naphthoxy radical self-reaction. *Environmental Science & Technology*, *46*(21), 11,813–11,820. <https://doi.org/10.1021/es302841j>
- Huang, R. J., Zhang, Y., Bozzetti, C., Ho, K. F., Cao, J. J., Han, Y., et al. (2014). High secondary aerosol contribution to particulate pollution during haze events in China. *Nature*, *514*(7521), 218–222. <https://doi.org/10.1038/nature13774>
- Huneus, N., Schulz, M., Balkanski, Y., Griesfeller, J., Prospero, J., Kinne, S., et al. (2011). Global dust model intercomparison in AeroCom phase I. *Atmospheric Chemistry and Physics*, *11*(15), 7781–7816. <https://doi.org/10.5194/acp-11-7781-2011>
- Krueger, B. J., Grassian, V. H., Cowin, J. P., & Laskin, A. (2004). Heterogeneous chemistry of individual mineral dust particles from different dust source regions: The importance of particle mineralogy. *Atmospheric Environment*, *38*(36), 6253–6261. <https://doi.org/10.1016/j.atmosenv.2004.07.010>
- Li, L., Huang, Z., Dong, J., Li, M., Gao, W., Nian, H., et al. (2011). Real time bipolar time-of-flight mass spectrometer for analyzing single aerosol particles. *International Journal of Mass Spectrometry*, *303*(2-3), 118–124. <https://doi.org/10.1016/j.ijms.2011.01.017>
- Li, L., Li, M., Huang, Z., Gao, W., Nian, H., Fu, Z., et al. (2014). Ambient particle characterization by single particle aerosol mass spectrometry in an urban area of Beijing. *Atmospheric Environment*, *94*, 323–331. <https://doi.org/10.1016/j.atmosenv.2014.03.048>
- Li, N., Long, X., Tie, X., Cao, J., Huang, R., Zhang, R., et al. (2016). Urban dust in the Guanzhong basin of China, part II: A case study of urban dust pollution using the WRF-Dust model. *Science Of The Total Environment*, *541*, 1614–1624. <https://doi.org/10.1016/j.scitotenv.2015.10.028>
- Liu, L. Y., Shi, P. J., Gao, S. Y., Zou, X. Y., Erdon, H., Yan, P., et al. (2004). Dustfall in China's western loess plateau as influenced by dust storm and haze events. *Atmospheric Environment*, *38*(12), 1699–1703. <https://doi.org/10.1016/j.atmosenv.2004.01.003>
- Long, X., Li, N., Tie, X., Cao, J., Zhao, S., Huang, R., et al. (2016). Urban dust in the Guanzhong Basin of China, part I: A regional distribution of dust sources retrieved using satellite data. *Science of the Total Environment*, *541*, 1603–1613. <https://doi.org/10.1016/j.scitotenv.2015.10.063>
- Moffet, R. C., de Foy, B., Molina, L. T., Molina, M. J., & Prather, K. A. (2008). Measurement of ambient aerosols in northern Mexico City by single particle mass spectrometry. *Atmospheric Chemistry and Physics*, *8*(16), 4499–4516. <https://doi.org/10.5194/acp-8-4499-2008>
- Qin, X., Bhave, P. V., & Prather, K. A. (2006). Comparison of two methods for obtaining quantitative mass concentrations from aerosol time-of-flight mass spectrometry measurements. *Analytical Chemistry*, *78*(17), 6169–6178. <https://doi.org/10.1021/ac060395q>
- Qin, X., Pratt, K. A., Shields, L. G., Toner, S. M., & Prather, K. A. (2012). Seasonal comparisons of single-particle chemical mixing state in Riverside, CA. *Atmospheric Environment*, *59*, 587–596. <https://doi.org/10.1016/j.atmosenv.2012.05.032>
- Seinfeld, J. H., & Pandis, S. N. (2016). *Atmospheric chemistry and physics: From air pollution to climate change*. Hoboken, NJ: John Wiley & Sons.
- Silva, P. J., Carlin, R. A., & Prather, K. A. (2000). Single particle analysis of suspended soil dust from Southern California. *Atmospheric Environment*, *34*(11), 1811–1820. [https://doi.org/10.1016/S1352-2310\(99\)00338-6](https://doi.org/10.1016/S1352-2310(99)00338-6)
- Silva, P. J., Liu, D.-Y., Noble, C. A., & Prather, K. A. (1999). Size and chemical characterization of individual particles resulting from biomass burning of local Southern California species. *Environmental Science & Technology*, *33*(18), 3068–3076. <https://doi.org/10.1021/es980544p>
- Song, X.-H., Hopke, P. K., Fergenson, D. P., & Prather, K. A. (1999). Classification of single particles analyzed by ATOFMS using an artificial neural network, ART-2A. *Analytical Chemistry*, *71*(4), 860–865. <https://doi.org/10.1021/ac9809682>
- Spencer, M. T., & Prather, K. A. (2006). Using ATOFMS to determine OC/EC mass fractions in particles. *Aerosol Science and Technology*, *40*(8), 585–594. <https://doi.org/10.1080/02786820600729138>
- Sullivan, R. C., Guazzotti, S., & Prather, K. A. (2005). *Kinetics of the simultaneous uptake of nitric acid on mineral dust and sea salt aerosols measured by ATOFMS*, Abstracts of Papers of the American Chemical Society (Vol. 229, pp. U127–U127). Washington, DC: American Chemical Society.
- Sullivan, R. C., Guazzotti, S. A., Sodeman, D. A., & Prather, K. A. (2007). Direct observations of the atmospheric processing of Asian mineral dust. *Atmospheric Chemistry and Physics*, *7*(5), 1213–1236. <https://doi.org/10.5194/acp-7-1213-2007>
- Sullivan, R. C., Guazzotti, S. A., Sodeman, D. A., Tang, Y., Carmichael, G. R., & Prather, K. A. (2007). Mineral dust is a sink for chlorine in the marine boundary layer. *Atmospheric Environment*, *41*(34), 7166–7179. <https://doi.org/10.1016/j.atmosenv.2007.05.047>
- Sullivan, R. C., & Prather, K. A. (2007). Investigations of the diurnal cycle and mixing state of oxalic acid in individual particles in Asian aerosol outflow. *Environmental Science & Technology*, *41*(23), 8062–8069. <https://doi.org/10.1021/es071134g>
- Tang, M., Cziczo, D. J., & Grassian, V. H. (2016). Interactions of water with mineral dust aerosol: Water adsorption, hygroscopicity, cloud condensation, and ice nucleation. *Chemical Reviews*, *116*(7), 4205–4259. <https://doi.org/10.1021/acs.chemrev.5b00529>
- Tang, M., Huang, X., Lu, K., Ge, M., Li, Y., Cheng, P., et al. (2017). Heterogeneous reactions of mineral dust aerosol: Implications for tropospheric oxidation capacity. *Atmospheric Chemistry and Physics*, *17*(19), 11,727–11,777. <https://doi.org/10.5194/acp-17-11727-2017>

- Tao, S., Wang, X., Chen, H., Yang, X., Li, M., Li, L., & Zhou, Z. (2011). Single particle analysis of ambient aerosols in Shanghai during the World Exposition, 2010: Two case studies. *Frontiers of Environmental Science & Engineering in China*, 5(3), 391–401. <https://doi.org/10.1007/s11783-011-0355-x>
- Tobo, Y., Zhang, D., Matsuki, A., & Iwasaka, Y. (2010). Asian dust particles converted into aqueous droplets under remote marine atmospheric conditions. *Proceedings of the National Academy of Sciences of the United States of America*, 107(42), 17,905–17,910. <https://doi.org/10.1073/pnas.1008235107>
- Toner, S. M., Shields, L. G., Sodeman, D. A., & Prather, K. A. (2008). Using mass spectral source signatures to apportion exhaust particles from gasoline and diesel powered vehicles in a freeway study using UF-ATOFMS. *Atmospheric Environment*, 42(3), 568–581. <https://doi.org/10.1016/j.atmosenv.2007.08.005>
- Usher, C. R., Al-Hosney, H., Carlos-Cuellar, S., & Grassian, V. H. (2002). A laboratory study of the heterogeneous uptake and oxidation of sulfur dioxide on mineral dust particles. *Journal of Geophysical Research*, 107(D23), 4713. <https://doi.org/10.1029/2002JD002051>
- Usher, C. R., Michel, A. E., & Grassian, V. H. (2003). Reactions on mineral dust. *Chemical Reviews*, 103(12), 4883–4940. <https://doi.org/10.1021/cr020657y>
- Wang, H. C., Lu, K. D., Chen, X. R., Zhu, Q. D., Chen, Q., Guo, S., et al. (2017). High N2O5 concentrations observed in urban Beijing: Implications of a large nitrate formation pathway. *Environmental Science & Technology Letters*, 4(10), 416–420. <https://doi.org/10.1021/acs.estlett.7b00341>
- Wang, Y. C., Huang, R. J., Ni, H. Y., Chen, Y., Wang, Q. Y., Li, G. H., et al. (2017). Chemical composition, sources and secondary processes of aerosols in Baoji city of northwest China. *Atmospheric Environment*, 158, 128–137. <https://doi.org/10.1016/j.atmosenv.2017.03.026>
- Wang, Y. Q., Zhang, X. Y., & Arimoto, R. (2006). The contribution from distant dust sources to the atmospheric particulate matter loadings at XiAn, China during spring. *Science of the Total Environment*, 368(2-3), 875–883. <https://doi.org/10.1016/j.scitotenv.2006.03.040>
- Wu, F., Chow, J. C., An, Z., Watson, J. G., & Cao, J. (2011). Size-differentiated chemical characteristics of Asian paleo dust: Records from Aeolian deposition on Chinese Loess Plateau. *Journal of the Air & Waste Management Association*, 61(2), 180–189. <https://doi.org/10.3155/1047-3289.61.2.180>
- Yang, F., Chen, H., Wang, X., Yang, X., Du, J., & Chen, J. (2009). Single particle mass spectrometry of oxalic acid in ambient aerosols in Shanghai: Mixing state and formation mechanism. *Atmospheric Environment*, 43(25), 3876–3882. <https://doi.org/10.1016/j.atmosenv.2009.05.002>
- Zelenyuk, A., Imre, D., Wilson, J., Zhang, Z., Wang, J., & Mueller, K. (2015). Airborne single particle mass spectrometers (SPLAT II & miniSPLAT) and new software for data visualization and analysis in a geo-spatial context. *Journal of the American Society for Mass Spectrometry*, 26(2), 257–270. <https://doi.org/10.1007/s13361-014-1043-4>
- Zhang, G., Bi, X., Lou, S., Li, L., Wang, H., Wang, X., et al. (2014). Source and mixing state of iron-containing particles in Shanghai by individual particle analysis. *Chemosphere*, 95, 9–16. <https://doi.org/10.1016/j.chemosphere.2013.04.046>
- Zhang, R., Wang, G., Guo, S., Zamora, M. L., Ying, Q., Lin, Y., et al. (2015). Formation of urban fine particulate matter. *Chemical Reviews*, 115(10), 3803–3855. <https://doi.org/10.1021/acs.chemrev.5b00067>
- Zhang, T., Cao, J., Tie, X., Shen, Z., Liu, S., Ding, H., et al. (2011). Water-soluble ions in atmospheric aerosols measured in Xi'an, China: Seasonal variations and sources. *Atmospheric Research*, 102(1-2), 110–119. <https://doi.org/10.1016/j.atmosres.2011.06.014>
- Zhang, X. X., Shi, P. J., Liu, L. Y., Tang, Y., Cao, H. W., Zhang, X. N., et al. (2010). Ambient TSP concentration and dustfall in major cities of China: Spatial distribution and temporal variability. *Atmospheric Environment*, 44(13), 1641–1648. <https://doi.org/10.1016/j.atmosenv.2010.01.035>